بسم الله الرحمن الرحيم

Sudan University of Science and Technology

College of Graduate Studies

Estimation of Pediatric Patient's Radiation Dose During Nuclear Medicine Test

تقييم الجرعة الاشعاعية للأطفال المرضى أثناء فحوصات الطب النووي

A thesis submitted in partial fulfillment for the requirements

of Master degree in Nuclear Medicine Sciences

By:

Mayada Abazar Suliman Elmakki

Supervisor

Prof.Dr. Mohamed Elfadil Mohamed

2021

قال تعالى:

﴿ إِنَّا فَتَحْنَا لَكَ فَتْحًا مُبِينًا ﴾

سورة الفتح الآية ﴿1﴾

Dedication

I am honored to dedicate this compilation to my parents. The two people who gave me the main tools and values by them I am standing today.
Words may never be enough to thank my father and my mother for all the opportunities they have offered for me.

To my friends....

Mama and papa: I hope that I can make you proud.

Acknowledgements

This project would not have been possible without the guidance and the help of several individuals who in one way or another contributed and extended their valuable assistance in the preparation and completion of this portfolio.

First and foremost, my utmost appreciation to Dr. Suhaib Mohamed Salih who gave me the golden opportunity to do this compilation and for his professional guidance and valuable support.

I would like to express also my special thanks and gratitude to my family who supported me morally and financially. Especially to my beloved sister (Meaad) who is always ready to support me.

Last but not the least the on above all of us the omnipotence ,omniscience and omnipresent god, for answering my prayers for giving me that strength and wisdom , thank you so much "Allah".

"Thanks again to all of who helped me. God Bless us forever”

Abstract

Estimate of effective dose for pediatric in Khartoum state for three nuclear medicine scan the thyroid, Kidney (dynamic renal scan with DTPA) and bone using descriptive, analytic and cross sectional method in the research. the average of effective dose to all patients according to their age, for age group from 1-3 years old the mean for thyroid was 1.2 mSv, for dynamic renal scan 0.73 mSv and for bone scan it was 3.45 mSv. For age group 4-8 years old the mean for thyroid was 2.84 mSv, for dynamic renal scan 0.80 mSv and for bone scan it was 3.32 mSv. For age group 9-13 years old the mean for thyroid was 2.22 mSv, for dynamic renal scan 0.82 mSv and for bone scan it was 3.35 mSv. For age group 14-17 years old the mean for thyroid was 1.85 mSv, for dynamic renal scan 0.76 mSv and for bone scan it was 3.45 mSv. **And** the comparison between present study with other studies according to ED where for thyroid the present study was 2.03 mSv while in ARPANSA 2008 study it was 2.2 mSv which consider higher than our present study. For dynamic renal scan present study was 0.78 mSv while in ARPANSA 2008 study was 6 mSv which consider higher than our present study while in Silvia Maria 2014 study was 0.75 mSv which consider lower than our present study. For bone present study was 3.39 mSv while in ARPANSA 2008 study was 5.5 mSv which consider higher than our present study.

ملخص البحث

تقدير الجرعة الفعالة للأطفال بولاية الخرطوم لثلاث أنواع من فحوصات الطب النووي، للغدة الدرقية والكلى والعظام وكان متوسط الجرعة الفعالة لجميع المرضى حسب أعمارهم ، للفئة العمرية من 1-3 سنوات متوسط الغدة الدرقية كان 1.2 ملي سيفرت ، و للكلى 0.73 ملي سيفرت ، ولمسح العظام كان 3.45 ملي سيفرت. بالنسبة للفئة العمرية من 4 إلى 8 سنوات ، كان متوسط الغدة الدرقية 2.84 ملي سيفرت ، و للكلى 0.80 ملي سيفرت ، وبالنسبة لمسح العظام كان 3.32 ملي سيفرت. بالنسبة للفئة العمرية من 9 إلى 13 عامًا ، كان متوسط الغدة الدرقية 2.22 ملي سيفرت ، وللكلى 0.82ملي سيفرت ، وبالنسبة لمسح العظام كان 3.35 ملي سيفرت. بالنسبة للفئة العمرية 14-17 سنة ، كان متوسط الغدة الدرقية 1.85 ملي سيفرت ، وللكلى 0.76 ملي سيفرت ، وبالنسبة لمسح العظام كان 3.45 ملي سيفرت. والمقارنة بين الدراسة الحالية والدراسات الأخرى وفقًا للجرعه الفعاله حيث كانت الدراسة الحالية للغدة الدرقية 2.03 ملي سيفرت بينما في دراسة ARPANSA 2008كانت 2.2 ملي سيفرت والتي تعتبر أعلى من دراستنا الحالية. بالنسبة إلى للكلى كانت الدراسة الحالية 0.78 ملي سيفرت بينما كانت الدراسة في ARPANSA 2008 6 ملي سيفرت والتي تعتبر أعلى من دراستنا الحالية بينما كانت دراسة سيلفيا ماريا 2014 0.75 ملي سيفرت والتي تعتبر أقل من دراستنا الحالية. بالنسبة للعظام ، كانت الدراسة الحالية 3.39 ملي سيفرت بينما كانت الدراسة في ARPANSA 2008 5.5 ملي سيفرت والتي تعتبر أعلى من دراستنا الحالية.

Contents

List of tables

List of figures

List of abbreviation

A	Activity
Avg. ED	Average Effective Dose
Bq	Becquerel
BSA	Body Surface Area
CT	Computed Tomography
Ci	Curie
D	Absorbed dose
DMSA	Di-Mercapto-Succinic Acid
DTPA	Diethylene Triamine Pentaacetic Acid
DICOM	Digital Imaging and Communications in Medicine
ED	Effected Dose
EANM	European Association of Nuclear Medicine
FOV	Field of view
Gy	Grey
HEU	Highly Enriched Uranium-235
HT, R	Equivalent dose
IAEA	International Atomic Energy Agency
IR	Radiation
J	Joule
kVP	kilovolt-Peak
KeV	Kilo Electron Volt
LAO	Left Anterior Oblique

LEU	Low Enriched Uranium-235
LEHR	Low Energy High Resolution
LLATs	Left Lateral
LPO	Left Posterior Oblique
m	Mass
Max	Maximium
MBq	Mega biqueral
mCi	Milli curie
MDP	Methylene Diphosphonate
Min	Minimum
mrem	Millirem
N	Newton
NM	Nuclear medicine
NMGI	Nuclear Medicine Global Initiative
PACS	Picture Archiving And Communications Systems
PET	Positron Emission Tomography
PHA	Pulse Height Analyzer
PMT	Photomultiplier Tube
R	Roentgens
RAO	Right Anterior Oblique
RBE	Relative Biological Effectiveness
Rec A	Recommended Activity
RLATs	Right Lateral
RPO	Right Posterior Oblique

STD	Standard Deviation
STP	Standard Temperature And Pressure
SPECT	Single-Photon Emission Computed Tomography
Sv	Sieverts
T	Time
Tc	Technetium
$^{99m}TcO_4$	Technetium pertichnitate
TLD	Thermo luminescent dosimetry
Wt.	Weight
WHO	World health organization
X	Exposure

Chapter one

Introduction

1.1 Introduction:

The science of nuclear medicine (NM) involves the administration of trace quantities of radionuclide's that are used to provide diagnostic information in a diverse range of diseases. In its most basic form, a NM study comprises of injecting a radiopharmaceutical, a combination of specific pharmaceutical tagged with a gamma-ray-emitting radioactive tracer into the body. There are a number of pharmaceutical available which are used for specific organ imaging. It function is to carry gamma emitting radioisotope into a specific organ. When the radionuclide decays, gamma rays photons are emitted. The energy of these gamma photons is such that a large number of photons are exited from the body without being scattered or attenuated. These photons are later detected by a position-sensitive instruments called gamma camera or scintillation camera and form an image of the distribution of the radionuclide, and hence the compound to which it was attached (Shahzad 2019).

1.2 Gamma camera

Gamma cameras are based on the detection of gamma rays emitted from radionuclides. Radionuclides can be ingested or injected into the body. The camera accumulates counts of gamma photons, which are detected by crystals in the camera. Just like an X-ray, the gamma camera will yield a two-dimensional projection of a three-dimensional object. A tomographic version of the gamma camera is called SPECT, which yields slices through the body. Because the detection techniques of gamma cameras and SPECT are based on the same concept, the same radioisotopes can be used for both techniques. Commonly used isotopes include technetium-99m, iodine-123, and indium-111. (Lars Johansson, 2015)

1.3 Biological effect of radiation on children

Exposures from the largest nuclear disasters in human history—first in Hiroshima and soon after in Nagasaki—provided clear evidence that ionizing radiation (IR) is a human carcinogen. Significant increases in blood, breast, and other cancers have been observed in A-bomb survivors. The results of these epidemiological studies have also demonstrated that exposure to IR during childhood may result in an increased excess risk of cancer compared to adults, pointing towards higher sensitivity to radiation-induced cancers in children. Among exposed children, the incidence of leukemia rose dramatically just a few years after exposure. Studies from Chornobyl (Ukrainian transliteration) further expanded our knowledge on increased sensitivity of children to IR, as indicated by the substantial increase in the relative risk of thyroid cancer in children and adults who were exposed to high thyroid doses (over 1 Gy) in their childhood.

It is now generally accepted that children are more sensitive to radiation than adults, specifically with higher relative risk of cancers including leukemia, brain, breast, skin, and thyroid cancers following exposures. In part, this is because of the radiosensitivity of their developing organs and tissues. Also, the longer post-exposure life expectancy increases the lifetime risks of developing radiation-induced malignancies. This is becoming important because 70% to 80% of all children diagnosed with cancer have long-term survival. In this review, we will summarize the current knowledge on the risks of radiation-induced cancers as a consequence of pediatric exposures. (Kristy R. Kutanzi 2016)

1.4 Problem of the study

Most of pediatric patient received a higher dose during nuclear medicine imaging procedures.

1.5 Objective

General objective:

Reduce the quantity of the injected dose given to the pediatric patients.

Specific objective:

- To evaluate the pediatric effective dose.
- To estimate the dose according to weight and age.
- To calculate the dose according to type of study and radiopharmaceuticals used.
- To compare effective dose and present study.

Chapter two

Theoretical Background

2.1 Nuclear Medicine:

The discovery of x-rays on November 8 1895, was reported to the French Academy of Science in January 1896. One of its members was the physicist Henri Becquerel at Musee d'Histoire Naturelle in Paris. He had the impression that the new rays were generated from the point of the discharge tube which emitted fluorescent light when it was hit by cathode rays. This gave him the idea that other fluorescent materials might also emit the same type of radiation and he subsequently began a series of experiments in order to investigate this. He used a salt of uranium and potassium and was able to show that, after being exposed to sunlight, this substance emitted radiation which could penetrate black paper and blacken a photographic plate. He reported his findings to the Academy on February 24, 1896. He then intended to repeat his experiments but the sky over Paris was too cloudy for producing an effective excitement of fluorescence. On March I, he nevertheless developed his photographic plates expecting only a minor blackening, but the blackening was as deep as in his previous experiments. In his report to the Academy on March 2, 1896 he wrote; 'I shall particularly insist on the following fact, which appears to me very important and quite outside the range of the phenomena one might expect to observe. The same crystalline lamellas, placed opposite photographic plates, under the same conditions, separated by the same screen, but shielded from excitation by incident radiation and kept in darkness, still produce the same photographic impression. Becquerel’s discovery inspired several scientists to further research on this new phenomena (Sten Carlson 2005).

Marie and Pierre Curie named it radioactivity and tried to chemically isolate the substance which emitted the radiation. They then discovered two new elements, radium

and polonium. Ernest Rutherford at Cavendish Laboratory in Cambridge started his work to dissect the atom. He identified alpha- and beta particles. Together with F. Soddy he examined the temporal properties of the radioactive decay and the transformation of one element to another or a physically divergent form of the same element; isotopes as Soddy later named them. Rutherford and co-workers were able to show that the mass of an atom is concentrated in a small nucleus with the electrons occupying orbits around it. This formed the basis of the atom theory proposed by Niels Bohr in 1913. This was a very dynamic period in physics (Sten Carlson 2005).

Two main theories were formed: the theory of relativity proposed by A. Einstein and the quantum theory with M. Planck as the first in the line of several scientists in this field. The understanding of the structure of the atom and the nucleus subsequently increased. The neutron was discovered by J. Chadwick in 1932 and in 1934 F. Joliot and I. Curie were able to prove the production of an artificial radionuclide, (P-30) as a result of bombarding aluminum with neutrons from a radium-beryllium source. 'These experiments give the first chemical proof of artificial transmutation.

The possibility to produce artificial radionuclides was something the chemist George de Hevesy had long waited for. In 1911. When working under Rutherford at the Cavendish Laboratory, he developed the idea that a radioactive substance, chemically inseparable from a stable substance, could be used as an indicator of the latter. Together with F. Paneth he used this method to study the solubility of lead salts. This was the first application of radioactive tracers. De Hevesy also realized that this method could be used to study biological processes but the natural radionuclides available at this time were all so poisonous that such experiments were rendered impossible. He did, however, conduct one experiment where he observed how an isotope of lead was taken up and distributed in a plant (Vicia faba). In 1935, de Hevesy came to Niels Bohr's Institute in Copenhagen. His main interest was to find a radionuclide which could be used in biological research. He selected 32P and started a

series of experiments where different phosphorus compounds were given to animals in order to study the distribution and metabolism of the substances. Together with the Danish physician O. Chievitz, he published the first results in the journal 'Nature', in September 1935). This publication revealed new information about the metabolism of the skeleton. 'The results strongly support the view that the formation of bone is a dynamic process, the bones continuously taking up phosphorus atoms which are partly or wholly lost again and are replaced by other phosphorus atoms.', they wrote (Sten Carlson 2005).

2.2 Gamma Camera System

The gamma camera is the principal instrument for imaging in nuclear medicine and. As can be seen, it consists of a large detector in front of which the patient is positioned. Gamma cameras with more than one detector are now common, allowing a higher throughput of patients by acquiring two or more views simultaneously. Every aspect of the modern gamma camera is under computer control, allowing the operator to select the study acquisition time, or the number of counts to be acquired, to set the pulse height analyzers to reject scattered radiation, control the detector and patient bed positions for SPECT and whole body procedures, and display the image.

All gamma camera manufactures sell associated computers and software to process and display the acquired images. The type of computer and the operating system upon which the software functions has, in the past, varied between manufacturers. This has led to a number of problems, which has hindered the transfer of data between systems. However, in recent years, driven by the demand for onscreen reporting of images by clinicians and the need to transfer data to picture archiving and communications systems (PACS), these problems have, in part, been overcome. The solution has been to develop an industry standard data format (DICOM) which, when used with the correct software, will allow the free movement of data between imaging systems (Peter F. Sharp et al 2005).

2.2.1 Mode of Operation of the Gamma Camera

The image of the distribution of the gamma-ray-emitting radiopharmaceutical is produced in the scintillation crystal by a collimator. The gamma rays, which are not visible to the eye, are converted into flashes of light by the scintillation crystal. This light is, in turn, transformed into electronic signals by an array of photomultiplier tubes (PMT) viewing the rear face of the crystal. After processing, the outputs from the PMTs are converted into three signals, two of which (X and Y) give the spatial location of the scintillation while the third (Z) represents the energy deposited in the crystal by the gamma ray. To improve their quality these signals then pass through correction circuits. The Z signal goes to a pulse height analyzer (PHA), which tests whether the energy of the gamma ray is within the range of values expected for the particular radionuclide being imaged. If the Z signal has an acceptable value, then a signal is sent instructing the display to record that there has been a gamma ray detected, the position being determined by the X and Y signals (Peter F. Sharp et al 2005).

2.2.2 Collimator

It consists of a lead plate through which runs an array of small holes whose axes are perpendicular to the face of the collimator and parallel to each other. Only those gamma rays that travel along a hole axis will pass into the scintillation crystal, while those that approach the collimator at an oblique angle will hit the septa and be absorbed. The two main parameters describing collimator performance are spatial resolution and sensitivity. Resolution is a measure of the sharpness of the image and is approximately equal to the minimum separation needed between two structures if they are to be resolved. Typically the best spatial resolution that can be achieved with a camera fitted with a parallel-hole collimator is about 7 mm.

Sensitivity is a measure of the proportion of those gamma rays incident on the collimator that pass through to the detector; the higher the sensitivity, the greater the

count rate recorded. Typically the sensitivity for a parallel-hole collimator is only 0.1% (hence 99.9% of photons are absorbed by the collimator and do not reach the detector). The effectiveness of a collimator in producing an image in the scintillation crystal will depends upon the dimensions of the collimator (Peter F. Sharp et al 2005).

2.2.3 Detector

While the collimator modifies the gamma ray flux so as to create an image, it is the function of the detector assembly to convert the gamma rays into a form that will, eventually, allow a visible image to be produced. This process takes place in two stages. The first step is the conversion of the gamma rays into visible light by means of a **scintillation crystal**, the scintillation crystal used in gamma cameras is made from sodium iodide with trace quantities of thallium added, NaI (Tl). The second these scintillations are turned into electrical signals by the **PMTs.** The PMTs are usually arranged in a close packed array to ensure that the smallest possible gaps are left between tubes. In recent years, the shape of the crystal has changed from circular to rectangular, as the latter is more suitable for imaging the body. Typically, the crystal size is 60 × 45 cm, giving a field of view of about 55 × 40 cm.

About 60 PMTs are needed to cover this rectangular crystal. While PMTs with a photocathode diameter of 3 inches are used mainly, it is also necessary to use some 2 inch diameter tubes.

The PMT not only converts light into an electronic signal but also, as its name suggests, magnifies the electronic signal (typically by a factor of 107) to give a sufficiently large current for the subsequent electronics. Even with this signal amplification pre-amplifiers built into the PMT are necessary to ensure a sufficient signal-to-noise ratio (Peter F. Sharp et al 2005).

2.2.4 Analogue Systems

The signals from the PMTs are processed to give the three signals required, X and Y providing spatial information and Z the energy. The energy signal is produced simply by summing the outputs from all of the tubes, so measuring the total light produced by the scintillation. The spatial information is more difficult to produce. What is required is that the processed signal should be proportional to the X or Y location of the scintillation. This is achieved by weighting the signals from each tube by passing the output from the PMTs through resistors or capacitors (Peter F. Sharp et al 2005).

2.2.5 Digital Systems

Modern camera systems now rely heavily on digital technology, both for correction of the spatial, energy, and temporal information and for the analysis of image data. Since this requires the analogue signal to be digitized, there is a strong case for having a completely digital camera. Two general approaches are currently taken; either to digitize the X, Y, and Z signals immediately after these have been computed by analogue circuitry or, in the latest generation of cameras, to completely replace the analogue circuits, the signals from the PMTs being digitized before the X, Y, and Z signals are computed. In the latter case each PMT has an analogue to digital converter located after the preamplifier, and the signal position is calculated from the centroid of the signals from a group of PMTs, usually chosen to be those having the strongest and hence least noisy signals. The Z signal is calculated by summing the outputs from the group of tubes (Peter F. Sharp et al 2005).

2.2.6 Pulse Height Analysis

The collimator is responsible for creating an image out of the flux of gamma rays incident on it, yet not all of these gamma rays will carry useful image information. In particular, those rays that have been Compton scattered in the patient, and so appear to come from another location, simply reduce image contrast. Such rays can be identified

by the fact that in being scattered they also lose energy, the amount being dependent on the angle through which they were deviated. As the scintillation detector allows the energy deposited by the gamma ray in the crystal to be measured, this information can be used to exclude scattered gamma rays. However, as has already been mentioned, the gamma camera is limited in the accuracy with which it can measure energy, with the result that even in the absence of scatter the gamma rays appear to have a range of energies. The width of this so-called photopeak spectrum, measured at half the maximum height, is about 10% of the true energy. The pulse height analyzer allows the operator to select only the signals from those gammas in which the height of the Z signal, that is, gamma ray energy, has a certain value or range of values. If many useful gammas are not to be excluded from the image, a range of energies must be allowed through the PHA, and typically a window equal to 20% of the peak energy value is used; i.e. for 99mTc with a gamma ray of 140 keV those signals with energies between 126 and 154 keV are judged to be acceptable (Peter F. Sharp et al 2005).

While the scattered gamma rays are distinguishable by their lower energy, the spreading out of the photopeak spectrum may mean that the energy of un scattered gammas overlaps that of scattered ones. This overlap of the Compton and photopeak spectrum means that a choice must be made between using a narrow window and so excluding a large proportion of unscattered rays or accepting the presence of some scattered radiation in the image. Usually the latter is chosen, and with a 20% Windows bout30%of the gamma rays in the image will have been scattered.

When using radionuclides that emit gamma rays at different energies, multiple window analyzers need to be employed. Typically a maximum of three sets of windows is available. In this instance, it is important to remember that scattered radiation from the higher-energy gammas may overlap into the lower-energy photopeaks and this may influence which gamma ray energies should be selected (Peter F. Sharp et al 2005).

2.2.7 Correction Circuits

To improve image quality, real-time compensation is provided for some of the defects in camera performance mentioned above. It is, however, only possible to correct where the cause of the distortion is not random. So, while non-linearity can be corrected, it is not possible to improve the intrinsic spatial resolution of the camera (Peter F. Sharp et al 2005).

2.2.8 Image Display

Modern camera systems employ digital display systems. If the Z signal corresponding to a particular detected gamma ray falls within the window that has been set on the PHA, then an enable signal is sent and the X and Y signals are recorded. The most common form of image acquisition is called matrix or frame mode. The camera's field of view is divided into a regular matrix of picture elements or pixels. Each pixel is assigned a unique memory location in the computer. The value stored in this location is the number of gamma ray events that have been detected in the corresponding location on the camera face. The number, and hence the size, of the pixels used is of practical importance and depends on (i) the available computer memory (unlikelyto be a problem withmodern systems), (ii) the total number of images to be acquired, (iii) the number of counts contained in each image, and (iv) the required temporal and spatial resolution.

As modern systems can acquire and display static images with array sizes of up to 2048×2048 pixels, image quality is comparable with that of analogue images. Each pixel is typically stored as a 16 bit unsigned integer (allowing count values to range from 0 to 65 535); more bits per pixel would allow higher counts to be recorded, but at the expense of storage space, image transfer rate, and possibly processing time.

The image data are mapped from the array of numbers, representing the number of gamma rays acquired at a specific spatial location, into a viewable image by a look-up table which links the number of gamma rays to a specific value of displayed image

intensity. The first question to be addressed is how best to represent image intensity, both gray shades and colors having been used. The human eye can distinguish thousands of different colors, compared with only several tens of gray shades. The use of color to display intensity information, known as pseudo color, should therefore permit a much wider dynamic range to be reproduced (Peter F. Sharp et al 2005).

2.3 Mo-99 Production Process

There are two primary approaches for producing the medical isotope Mo-99: fission of U-235, which produces Mo-99 and other medically important isotopes such as I-131 and Xe-133, and neutron capture by Mo-98 to produce Mo-99. This section provides an overview of this production method and is organized in terms of the following three processes:

2.3.1 Fabrication of uranium targets

The target used for Mo-99 production is a material containing uranium-235 that is designed to be irradiated in a nuclear reactor. The target is designed to satisfy several requirements: First, it must be properly sized to fit into the irradiation position inside the reactor. Second, it must contain a sufficient amount of U-235 to produce the required amount of Mo-99 when it is irradiated. Third, it must have good heat transfer properties to prevent overheating (which could result in target failure) during irradiation. Fourth, the target must provide a barrier to the release of radioactive products, especially fission gases, during and after irradiation. Fifth, the target materials must be compatible with the chemical processing steps that will be used to recover and purify Mo-99 after the target is irradiated **(National Academies Press (US) 2009).**

2.3.2 Irradiation of targets in a nuclear reactor,

Mo-99 is produced in the uranium-bearing targets by irradiating them with thermal neutrons. Some of the U-235 nuclei absorb these neutrons, which can cause them to fission. The fission of the U-235 nucleus produces two but sometimes three lower-mass nuclei referred to as fission fragments. Approximately 6 percent of these fission fragments are Mo-99 atoms **(National Academies Press (US) 2009).**

2.3.3 Dissolution of the uranium target and recovery and purification of Mo-99.

Once the targets are removed from the reactor, they are cooled in water typically for half a day or less before being transported to the processing facility in shielded casks. Once at the processing facility, the targets are placed into hot cells for chemical processing. Processing is carried out quickly to recover the Mo-99 to minimize further losses from radioactive decay These three processes apply whether Mo-99 is produced from highly enriched uranium-235(HEU) or low enriched uranium-235(LEU) targets **(National Academies Press (US) 2009).**

The decay product of Mo-99 Tc-99m, is the workhorse isotope in nuclear medicine for diagnostic imaging. Tc-99m is used for the detection of disease and for the study of organ structure and function. Tc-99m is especially useful for nuclear medicine procedures because it can be chemically incorporated into small molecule ligands and proteins that concentrate in specific organs or tissues when injected into the body. The isotope has a half-life of about 6 hours and emits 140 keV photons when it decays to Tc-99, a radioactive isotope with about a 214,000-year half-life. This photon energy is ideally suited for efficient detection by scintillation instruments such as gamma cameras. The data collected by the camera are analyzed to produce detailed structural and functional images. **(National Academies Press (US) 2009).**

Tc-99m is currently produced through a multistep process that begins with the neutron irradiation of fissile U-235 contained in HEU or LEU targets in a nuclear reactor. This irradiation causes U-235 to fission and produces Mo-99 and many other fission products, including I-131 and Xe-133. Following irradiation, the targets are chemically processed to separate Mo-99 from other fission products. If desired, these other fission products can be recovered separately. The separated Mo-99, which is contained in a solution, is then adsorbed onto an alumina (Al_2O_3) column that is contained in cylinders that are about the diameter of a large pencil. The columns are shipped to radiopharmacies and hospitals in radiation-shielded cartridges known as technetium generators. The Mo-99 in the generators decays with about a 66-hour half-life to Tc-99m. The Tc-99m is typically recovered by passing a saline solution through the alumina column in the generator, a process known as eluting the generator. The saline removes the Tc-99m but leaves the Mo-99 in place. A technetium generator can be eluted several times a day for about a week before it needs to be replaced with a fresh generator **(National Academies Press (US) 2009).**

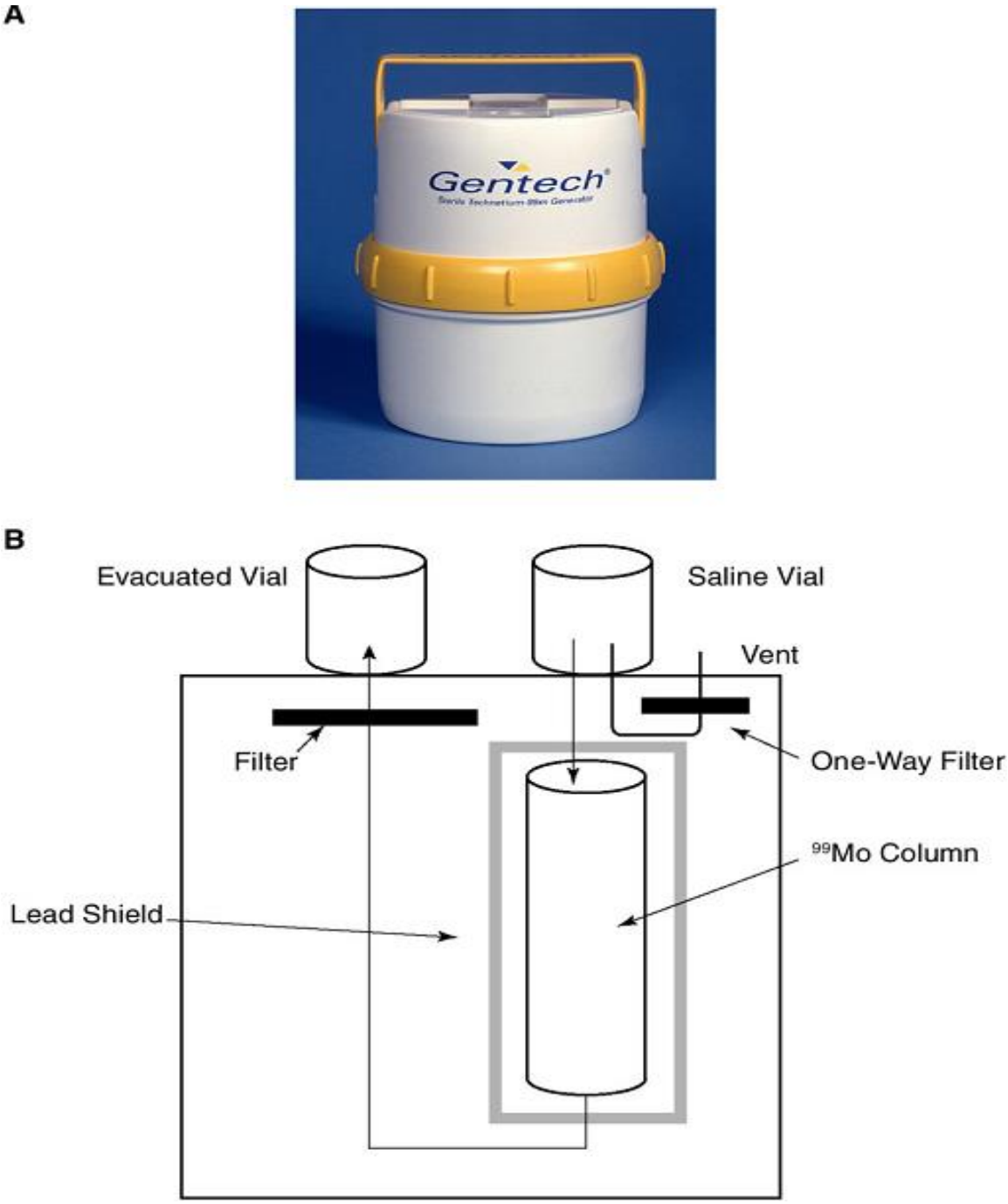

Figurs (2.1):

(a) External view of a technetium generator.

(b) Schematic diagram showing the internal structure of a typical technetium generator. **(National Academies Press (US) 2009).**

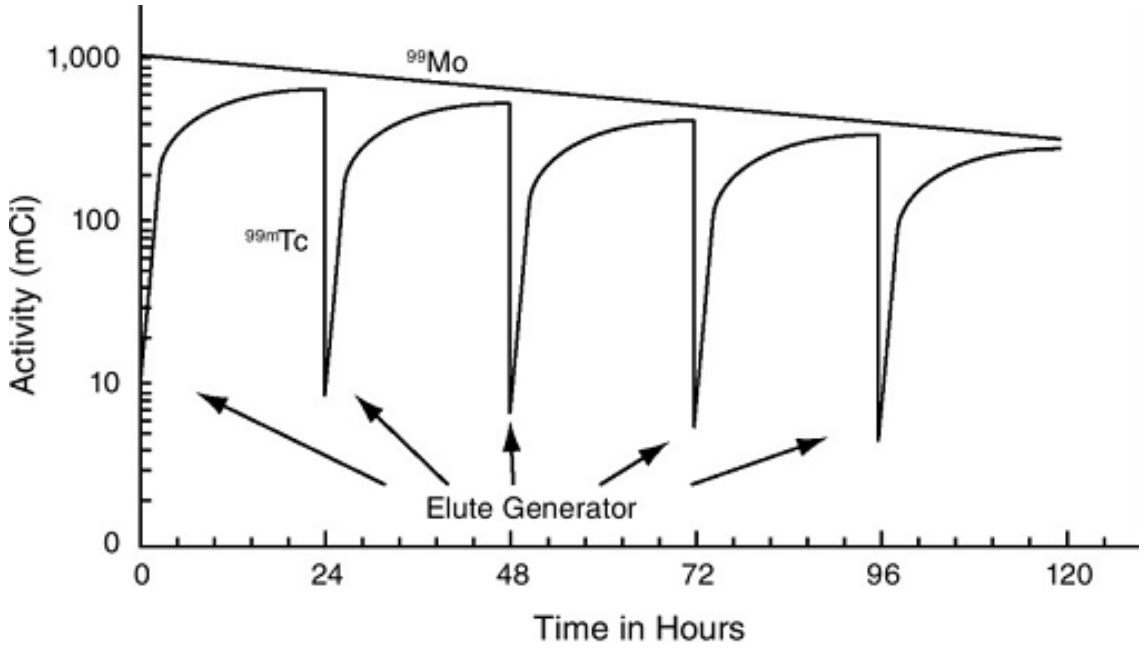

Figure (2.2): Plot of typical Mo-99 and Tc-99m activity on a logarithmic scale versus time for multiple elution of a technetium generator.

Because of its relatively short half-life (66 hours), Mo-99 cannot be stockpiled for use. It must be made on a weekly or more frequent basis to ensure continuous availability. The processes for producing Mo-99 and technetium generators and delivering them to customers are tightly scheduled and highly time dependent. An interruption at any point in the production, transport, or delivery of Mo-99 or technetium generators can have substantial impacts on patient care **(National Academies Press (US) 2009).**

2.4 Nuclear Medicine Diagnosis

2.4.1 Thyroid scan

Radiopharmaceuticals: 99mTcO4 (pertechnetate)

Adult Dose Range: $^{99m}TcO_4^-$: 2–10 mCi (74–370 MBq)

Method of Administration

^{99m}Tc by intravenous injection

Patient Preparation

- Identify the patient. Verify doctor's order. Explain the procedure.
- ^{99m}Tc: None other.
- Patient to discontinue thyroid medications and avoid contrast material.
- Refrain from eating foods containing iodine such as cabbage, turnips, greens, seafood, kelp, or large amounts of table salt.

Procedure (Usually Two Parts; Time: ~40 Minutes): $^{99m}TcO_4^-$

- Administer injection to patient; wait 15 to 20 minutes before imaging. Give patient water (optional lemon to clear salivary glands).
- Place patient in supine position with pillow under shoulders and chin up (Water's position).
- Using the LEHR collimator, obtain anterior views (300 seconds or 100,000 depending on protocol) with and without markers as per protocol (thyroid cartilage and suprasternal, marker strip, right side, etc.). RAO and LAO and perhaps a “pull-back” image (more distant) for ectopic thyroid tissue are optional images if a pinhole collimator is not available (Pete 2000)

2.4.2 Bone Scan

Radiopharmaceutical: MDP (methylene diphosphonate).

Adult Dose Range: 20–30 mCi (740–1110 MBq), pediatrics by weight.

Method of Administration: Intravenous.

Patient Preparation

- Identify the patient. Verify doctor's order. Explain the procedure.
- For flow of three phase bone study; remove any attenuating material from region of interest (ROI).
- Instruct patient to drink lots of fluids (hydrate well) and urinate often before imaging.
- Instruct patient to return in 2–4 hours (usually 3 hours) after injection for delayed statics, whole body imaging or SPECT.

Procedure (Time: Immediate Flows, ~10 Minutes; Scans, Acquired 2–4 Hours [Usually 3 Hours] After Injection; Images Take 20–60 Minutes)

- Instruc**t** patient to empty bladder, empty pockets, remove jewelry and necklaces, check pants and shirts for buttons, external prosthesis, braces, etc., anything that can cause artifacts and attenuation.
- Remove cardiac monitors from field of view (FOV).
- Note location of pacemaker, pumps, colostomy bags, etc.
- For whole body scan, position patient supine (although prone, sitting, or standing is not uncommon), arms at side, with knee pillow and foot band (if protocol) (Pete 2000).

2.4.3 Renal: Cortical Imaging (^{99m}Tc-DMSA)

Radiopharmaceutical: ^{99m}Tc-DMSA (dimercaptosuccinic acid)

Localization

- Compartmental, blood stream; DMSA: 90% binds to plasma proteins, 10% to 15% of injected dose remains bound to renal tubules.

Adult Dose Range: DMSA: 1–6 mCi (37–222 MBq),

Method of Administration: Direct intravenous injection or IV catheter with saline flush.

Patient Preparation

- Identify the patient. Verify doctor's order.
- Explain the procedure, especially the delay between injection and imaging.
- Patient is to be well hydrated and should void before test begins.

Procedure: (varies greatly; time: injection ~15 minutes, images ~45 minutes)

• Place patient in supine position, camera under table, except for kidney transplant patients for whom camera is placed above the abdomen. Prone for pinhole collimator, kidneys in field of view (FOV).

• Position camera with upper abdomen centered in FOV.

• Obtain images: Wide variation in protocols for imaging; 50% of injected DMSA dose is in kidneys within 1 hour.

• Inject, patient returns in 2–6 hours for delay imaging, and again for 24-hour delays if requested.

• Select imaging technique. Check with the radiologist.

• Optional images: 500,000–800,000 counts, posterior (at least). Some take RPOs and LPOs 30°, RLATs and LLATs, and/or anterior if horseshoe kidneys are suspected or kidney transplant. May need to magnify views for pediatric patients).

• Generate percent uptake for each kidney. Select posterior static taken at least at 1 hour. Software differs: some have automatic programs; some will allow regions of interest to be drawn, giving counts within area. Add two counts together for total, divide each by total to give percent uptake for each kidney: Combined percents should equal 100 (Pete 2000).

2.4.4 Dynamic Renal Imaging Techniques (Renogram)

Radiopharmaceutical: 99mTc-DTPA (diethylenetriaminepentaacetic acid)

Localization: Compartmental, blood flow

Adult Dose Range

• 99mTc: 3–20 mCi (111–740 MBq) generally 10mCi (370 MBq) for most studies.

Method of Administration: Bolus intravenous injection

Patient Preparation

• Identify the patient. Verify doctor's order. Explain the procedure.

• Instruct patient to hydrate well (water; up to 10 mL/kg) and void just before test.

• Post study voiding is recommended to lessen bladder exposure.

Procedure (VARIES GREATLY; TIME: ~30

• If GFR is to be included, count the syringe before and after injection for 1 minute at 20–30 cm from camera face (use same distance both times).

• Place patient in supine position, camera under table, except for kidney replacement patients for whom camera is placed anterior over the abdomen to include lower abdomen.

• Position camera by point source over xiphoid, umbilicus, pubic symphysis, and sides in field of view.

• Bolus intravenous injection, start camera. Note: some wait until they see activity blush in abdomen (the "umbrella" effect caused by the heart-liver-spleen and descending aorta) before starting camera. To be sure, set flow for 120 seconds; start camera just before injection.

• Diuretic (furosemide) study, use following options:

• Insert intravenous butterfly with 3-way stopcock, inject furosemide, flush and inject a bolus of radiotracer. Protocols vary for furosemide injection time. Some wait until 10 to 15 minutes for obstruction studies.

• For 1-minute flow: Inject bolus, start camera, inject furosemide, and flush.

• Acquire statics at 2- to 5-minute intervals for 30 minutes or serial (dynamic) 1-minute images for 30 minutes. (Most systems have a preset for renogram, renal qualitative or renal perfusion.) (Pete 2000).

2.4.5 Lymphoscintigraphy

Radiopharmaceutical: • 99mTc-sulfur colloid (filtered)

Localization

• Compartmental, phagocytosis. Particles are cleared by lymphatic system, 30% at3 hours.

Adult Dose Range: 200 μCi to 2 mCi (7.4–74 MBq);

Method of Administration

• For lymphedema: Injections, two sites per limb, subcutaneous, producing a wheal, placed into the web between fingers or toes depending on the area of interest.

Patient preparation

• Identify the patient. Verify doctor's order. Explain the procedure.

• Wipe area with alcohol pad, shave if necessary; clean area with Betadine or chosen sterilizing solution.

• For lymphedema, physician to instruct patient to wear elastic stockings. These should be removed 3–4 hours before study.

Procedure (procedures vary greatly; see sample protocols; time: ~1–6 hours)

• Prepare the area of interest for the patient (e.g., shave, alcohol wipe, Betadine).

• Lymphedema: Patient is injected subcutaneously in webs of feet or hands as indicated, two sites per limb.

• Place patient in prone, supine, or sitting position depending on location of site to best obtain images of lymph drainage.

• Immediate statics: 5–10 minutes per view, with or without markers or transmission images.

• Views: Anterior, posterior, obliques, and/or laterals to best image the direction of lymph node drainage.

• Marker images: Use a point source outlining the body and/or a transmission image using a 57Co flood source (cookie sheet) placed behind the patient to help define the position of the nodes of
Interest.

• Extremities: The inguinals or axillas should visualize within 10–30 minutes depending on how distal the site is. In these cases and trunk-oriented cancers, delays of the whole body (1–2 hours) may be required to visualize secondary drainage. Image in-transit nodes around knee(s) or elbow(s).

• Delays: 1–4 hours after injection (see Protocols below), use same views as before.

• Whole body: Sweep or statics to cover all drainage areas (Pete 2000).

2.5 Radiation Units:

The five basic concepts that relate a radiation worker to a source of radiation are (1) activity (A), measured in Becquerel's (Bq) or in curies (Ci); (2) exposure (X), measured in Coulombs/kg of air or in roentgens (R); (3) absorbed dose (D), measured in grays or in rads, (4) equivalent dose (H T), measured in sieverts or in rems, and (5) effective dose (E), also measured in sieverts or in rems (Max H. Lombardi 2007).

2.5.1 Activity

Activity is the number of radioactive atoms (N) decaying per unit time (t). The formal expression is

$$A = N/t$$

The S.I. unit of activity is the Becquerel (Bq), which is equal to one nuclear Transformation per second (1 nt/s). . The special or traditional units are the

$$\text{Curie} = 3.7 .10^{10} \text{nt/s}$$

2.5.2 Exposure (X)

Exposure is the sum of all the electrical charges (Q) of one sign produced by x- or gamma rays in a given mass (m) of dry air at standard temperature and pressure (STP). The formal expression for exposure is

$$X = Q/m$$

The S.I. unit of exposure is the Coulomb per kg (C/kg) of dry air at STP. The special unit of exposure is the roentgen (R), defined as $2.58. *10^{-4}$ C/kg of dry air at STP. This definition applies only to x- or gamma rays under 3 MeV of energy. One C/kg is equal to 3876 roentgens (Max H. Lombardi 2007).

2.5.3 Absorbed dose (D)

Absorbed dose (D) is the radiation energy (E) transferred to a unit mass (m) of any material. The formal expression is

$$D = E/m \quad (2.5)$$

The S.I. unit of absorbed dose is the gray (Gy), which is equal to the absorption of one joule of energy per kg of any material including the body of a patient or that of a technologist.

Reminder: In the macro world, the MKS system (meter, kilogram, second) is used. The unit of energy is the joule. One joule (J) = force of one newton (N) acting over a distance of one meter.

The special unit of absorbed dose is the rad (radiation absorbed dose), defined as the absorption of one hundredth of a joule per kg of any material or 1 rad = 0.01 J/kg of material.

To measure the absorbed dose by radiation workers, calibrated dosimeters are used. Examples are film badges and thermo luminescent dosimetry (TLD) badges to monitor body dose, and TLD ring dosimeters to monitor hand dose (Max H. Lombardi 2007).

2.5.4 Equivalent Dose (HT, R)

This concept replaces the former "dose equivalent," and was introduced to account for the differences in the ionizing quality of the various types of radiations. Equivalent dose is defined as the product of the average absorbed dose (DT,R) received by tissue (T) from radiation (R) times the radiation weighting factor (w R): HT,R= DT,R.wR(2.6)Average doses, DT,R, are expressed in grays (Gy) and equivalent doses, H T,R, are expressed in sieverts (Sv). Radiation weighting factors (w R) recommended by the NCRP are listed in Table 2.1. They replace the former quality factors (Q). The following example illustrates the concept of equivalent dose: A person accidentally inhales some radioactive dust. The absorbed dose to the respiratory tract is 50 mGy from alpha particles, 30 mGy from beta radiation, and 20 mGy from gamma rays.

The total absorbed dose is 50 + 30 + 20 = 100 mGy, but the equivalent dose takes into account the quality of each radiation by introducing the radiation weighting factors (w R) (Max H. Lombardi 2007).

2.5.5 Effective Dose (E)

Due to the fact that organs and tissues have different sensitivities to radiation, the concept of effective dose (E) was introduced and is defined as the sum of the products of the equivalent doses (H T, R) received by an organ times the tissue weighting factors (w T):

$$E = \Sigma (H\ T, R.\ w\ T)$$

Effective doses are also expressed in sieverts (Sv) (Max H. Lombardi 2007).

2.5.6 Relative biological effectiveness (RBE)

In radiobiology, the science that studies radiation effects on biological systems, the relative biological effectiveness (RBE) concept is used to account for the sensitivities of different biological systems to alpha radiation, beta radiation, electron beams, neutron fluxes of various energies and, of course, x- and gamma rays. RBE is the ratio of the dose of 250 kVP (kilovolt-peak) x-rays, which produces some effect, to the dose of another radiation that produces the same effect in the same degree. RBEs are useful to radiobiologists when they compare results of experiments done at different locations (Max H. Lombardi 2007)

2.6 Effect of radiation in pediatric

Estimating individual patient risk entails further understanding of individual organ dose with organ-specific risk coefficients adjusted for both patient age and sex. Radiation doses in diagnostic imaging are often presented in terms of "effective doses".

Effective dose is not appropriate for quantifying individual patient risk from the radiation dose of a particular medical imaging procedure. Only if the

patient populations are similar (with regard to both age and sex) can effective doses be of potential practical value for comparing relative examination doses (WHO 2016). The biological effects of radiation are derived principally from damage to DNA. The x-ray particle, a photon, releases energy when interacting with an electron. The electron may act either directly on DNA (direct action or affect) but may also interact on a water molecule resulting in a free radical, which in turn can damage DNA (indirect action or affect). The indirect effect is the more dominant effect, consisting of approximately 2/3 of photon interactions. DNA damage results in either single stranded breaks or double stranded breaks. Single stranded breaks are usually well repaired with minimum bio effects. Breaks in both strands of DNA (which are in close proximity) are more problematic to repair and underlie disruptive function that can result in cell death or in impaired cellular function resulting in the development of cancer. These inappropriate repairs with resultant stable aberrations can initiate one of the multi-step processes in radiation induced carcinogenesis. Of note, there are some chemicals, which serve as radio protectants, primarily in the setting of radiation oncology that have recently been reviewed. While not yet applicable to general diagnostic imaging, these DNA stabilizing agents provide a model for radiation protection at the cellular level.

Radiation results in two biological effects: deterministic and stochastic effects. For virtually all diagnostic imaging (CT, nuclear medicine, and radiography and fluoroscopy) radiation doses are at the levels which are stochastic. Stochastic effects are generally disruptions that result in either cancer or heritable abnormalities. For diagnostic imaging, the discussion is limited almost exclusively to the potential for cancer induction; heritable effects (i.e., on gametes) have not been shown to occur in diagnostic levels of

radiation in humans. For a stochastic effect, the risk increases with the dose but the severity of the effect (i.e., the severity of cancer) does not increase. There is also no threshold for this risk (see following discussion on models of radiation risks based on dose). The other biological effect is deterministic. Deterministic effects include cataracts, dermatitis (skin burns), and epilation (hair loss). With the deterministic effect, the amount of radiation determines the severity of effect. For example, the greater amount of radiation, the more extensive the hair loss. With deterministic effects, there is a threshold. Below this threshold the injury does not occur. Deterministic effects can be seen with extensive interventional procedures, and certainly with doses delivered from radiation oncology. Deterministic effects are, except for very unusual circumstances, including imaging errors, not encountered in during diagnostic medical imaging examinations (Donald P. Frush, 2013)

2.7 Previous study

Frederic H. Fahey (2015) study the Nuclear Medicine Global Initiative (NMGI) was formed in 2012 and consists of 13 international organizations with direct involvement in nuclear medicine. The underlying objectives of the NMGI were to promote human health by advancing the field of nuclear medicine and molecular imaging, encourage global collaboration in education, and harmonize procedure guidelines and other policies that ultimately lead to improvements in quality and safety in the field throughout the world. For its first project, the NMGI decided to consider the issues involved in the standardization of administered activities in pediatric nuclear medicine. This article presents part 1 of the final report of this initial project of the NMGI. It provides a review of the value of pediatric nuclear medicine, the current understanding of the carcinogenic risk of radiation as it pertains to the administration of radiopharmaceuticals in children, and the application of

dosimetric models in children. A listing of pertinent educational and reference resources available in print and online is also provided. The forthcoming part 2 report will discuss current standards for administered activities in children and adolescents that have been developed by various organizations and an evaluation of the current practice of pediatric nuclear medicine specifically with regard to administered activities as determined by an international survey of nuclear medicine clinics and centers. Lastly, the part 2 report will recommend a path forward toward global standardization of the administration of radiopharmaceuticals in children.

Frederic H. Fahey (2016) studied the practice of nuclear medicine in children is well established for imaging practically all physiologic systems but particularly in the fields of oncology, neurology, urology, and orthopedics. Pediatric nuclear medicine yields images of physiologic and molecular processes that can provide essential diagnostic information to the clinician. However, nuclear medicine involves the administration of radiopharmaceuticals that expose the patient to ionizing radiation and children are thought to be at a higher risk for adverse effects from radiation exposure than adults. Therefore it may be considered prudent to take extra care to optimize the radiation dose associated with pediatric nuclear medicine. This requires a solid understanding of the dosimetry associated with the administration of radiopharmaceuticals in children. Models for estimating the internal radiation dose from radiopharmaceuticals have been developed by the Medical Internal Radiation Dosimetry Committee of the Society of Nuclear Medicine and Molecular Imaging and other groups. But to use these models accurately in children, better pharmacokinetic data for the radiopharmaceuticals and anatomical models specifically for children need to

be developed. The use of CT in the context of hybrid imaging has also increased significantly in the past 15 years, and thus CT dosimetry as it applies to children needs to be better understood. The concept of effective dose has been used to compare different practices involving radiation on a dosimetric level, but this approach may not be appropriate when applied to a population of children of different ages as the radiosensitivity weights utilized in the calculation of effective dose are not specific to children and may vary as a function of age on an organ-by-organ bias. As these gaps in knowledge of dosimetry and radiation risk as they apply to children are filled, more accurate models can be developed that allow for better approaches to dose optimization. In turn, this will lead to an overall improvement in the practice of pediatric nuclear medicine by providing excellent diagnostic image quality at the lowest radiation dose possible.

Richard M. Shore (1986) found the most rational method for adjusting adult radiopharmaceutical dosages for children, four methods of dosage computation ware examined from the perspectives of diagnostic adequacy and radiation absorbed dose. For static imaging, information density is the most important factor in study quality, and adjustment of dosage by body weight (Wt.) for thick organs, and body surface area (BSA) for thin organs is recommended. Compared with adults, small children receive less radiation exposure if radiopharmaceutical dosages are adjusted by Wt., and slightly greater exposure if dosages are adjusted by BSA. For dynamic imaging studies, dosage requirements are governed by the spatial resolution needed for region of interest assignment, and the statistical reliability of the time-activity data. For dynamic renal imaging, renograms of similar quality are obtained if dosages are adjusted by height (Ht).Dynamic cardiac studies might appear to

require dosages even larger than those adjusted by Ht. which would result in higher radiation absorbed doses to pediatric patients. However, smaller dosages can be used in children by prolonging the imaging time and accepting lower temporal resolution. Dosage requirements for dynamic studies depend on which physiologic characteristics are measured from the time-activity data. Since the measurements of some characteristics demand higher count rates than others, dosage requirements ultimately depend on which measurements are clinically necessary. Close attention to the factors that determine these requirements may yield significant reduction in dosages, and thus in radiation exposure, for patients of all ages.

Jeffry A. Siegel (2017) A debate exists within the medical community on whether the linear no-threshold model of ionizing radiation exposure accurately predicts the subsequent incidence of radiogenic cancer. In this article, we evaluate evidence refuting the linear no-threshold model and corollary efforts to reduce radiation exposure from CT and nuclear medicine imaging in accord with the as-low-as-reasonably achievable principle, particularly for children. Further, we review studies demonstrating that children are not, in fact, more radiosensitive than adults in the radiologic imaging dose range, rendering dose reduction for children unjustifiable and counterproductive.

Efforts to minimize nonexistent risks are futile and a major source of

Persistent radiophobia. Radiophobia is detrimental to patients and parents, induces stress, and leads to suboptimal image quality and avoidance of imaging, thus increasing misdiagnoses and consequent harm while offering no compensating benefits.

Frederic H. Fahey(2011) The value of pediatric nuclear medicine is well established. Pediatric patients are referred to nuclear medicine from nearly all pediatric specialties including urology, oncology, cardiology, gastroenterology, and orthopedics. Radiation exposure is associated with a potential, small, risk of inducing cancer in the patient later in life and is higher in younger patients. Recently, there has been enhanced interest in exposure to radiation from medical imaging. Thus, it is incumbent on practitioners of pediatric nuclear medicine to have an understanding of dosimetry and radiation risk to communicate effectively with their patients and their families. This article reviews radiation dosimetry for radiopharmaceuticals and also CT given the recent proliferation of PET/CT and SPECT/CT. It also describes the scientific basis for radiation risk estimation in the context of pediatric nuclear medicine. Approaches for effective communication of risk to patients' families are discussed. Lastly, radiation dose reduction in pediatric nuclear medicine is explicated.

Chapter Three

Material and Methods

3.1 Material

3.1.1 Gamma camera

Figure 3.1: shows SPECT gamma camera dual head

3.1.1.1 Khartoum Oncology Hospital

Model: Nucline Spirit, SN: DH-506069-V0, Date of Manufacture: 2005

3.1.1.2 Royal Care International Hospital

Model: Nucline Spirit, SN: DH-004167-V, Date of Manufacture: 2010

Figure 3.2: shows SPECT gamma camera single head

3.1.1.3 Alnelain Medical Diagnostic Center

MiE medical imaging electronics (single head gamma camera)

Model DRBITER Digi37 WB, SN: 2008/43, Date of installation 2008

3.1.2 Dose calibrator

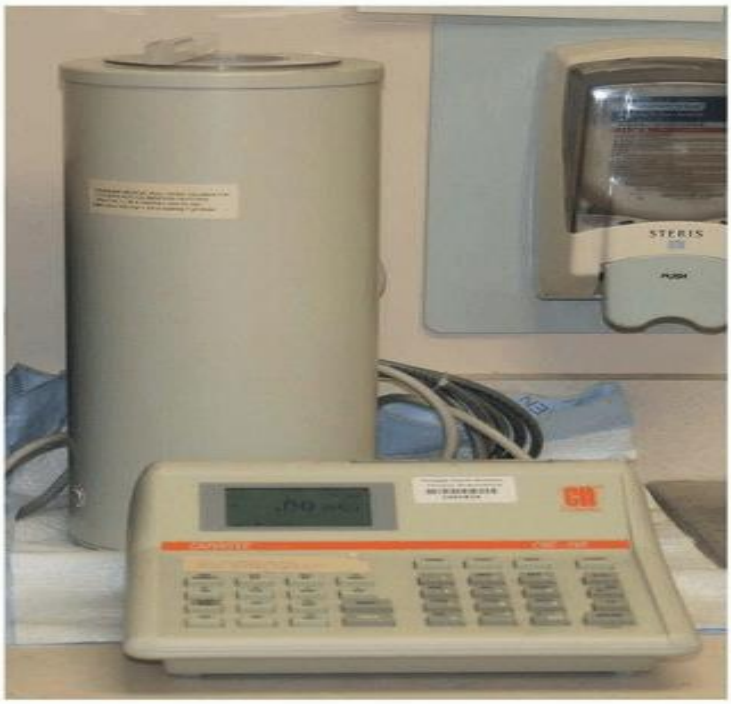

3.1.2.1 Alnelain Medical Diagnostic Center

Model: CRC-25R, SN: 250418, Date of installation: JULY 2008

3.1.2.2 Khartoum Oncology Hospital

Model: 0202020023, SN: 2012110023, Date of installation: 2011

3.1.2.3 Royal Care International Hospital

Atmolab 400 Dose Calibrator (BIOTEX)

Model: 086-335, SN: 10040102, Date of installation: Apr 2010

3.2 Method of data collection

The data was collected from each patient contain; gender, age, height, weight and administered dose**.**

All pediatric patient administered dose was calculated by the equation:

Pediatric dose = patient weight * adult dose/70

3.3 Calculation of effective dose

3.3.1 Dosage Calculator: Calculation of the administered activity in [MBq] and [mCi]
This card is based upon the publication by Jacobs F, Thierens H, Piepsz A, Bacher K, Van de Wiele C, Ham H, Dierckx RA. Optimized tracer-dependent dosage cards to obtain weight independent effective doses. Eur J Nucl Med Mol Imaging. 2005 May; 32(5):581-8.
This card summarizes the views of the Pediatric and Dosimetry Committees of the EANM and reflects recommendations for which the EANM cannot be held responsible. The dosage recommendations should be taken in context of „good practice "of nuclear medicine and do not substitute for national and international legal or regulatory provisions.

3.3.2 RADAR Medical Procedure Radiation Dose Calculator: and Consent Language Generator
For effective doses under 3 mSv (300 mrem), the risk is considered to be "minimal" and the consent language is rather brief. The doses are related to the equivalent number of days of exposure to natural background. For effective doses between 3 mSv (300 mrem) and 50 mSv (5000 mrem, or 5 rem), the risk is still termed "minimal", but slightly more consent form language is recommended. Doses are still related to the equivalent number of days of exposure to natural background, but information about individual organ doses should be given to the subject.'

3.4 Data analysis

The data was analyzed using Microsoft office (Excel 2019) and SPSS version 23.

3.5 Patients protocol in our study

3.5.1 Thyroid scan

Radiopharmaceuticals

• 99mTcO4 (pertechnetate)

Adult Dose Range

$^{99m}TcO_4^-$: 2–10 mCi (74–370 MBq)

Method of Administration

^{99m}Tc by intravenous injection

Patient Preparation

- Identify the patient. Verify doctor's order. Explain the procedure.
- ^{99m}Tc: None other.
- Patient to discontinue thyroid medications and avoid contrast material.
- Refrain from eating foods containing iodine such as cabbage, turnips, greens, seafood, kelp, or large amounts of table salt.

Procedure (Usually Two Parts; Time: ~40 Minutes)

$^{99m}TcO_4^-$

- Administer injection to patient; wait 15 to 20 minutes before imaging. Give patient water (optional lemon to clear salivary glands).
- Place patient in supine position with pillow under shoulders and chin up (Water's position).
- Using the LEHR collimator, obtain anterior views (300 seconds or 100,000 depending on protocol) with and without markers as per protocol (thyroid cartilage and suprasternal, marker strip, right side, etc.). RAO and LAO and perhaps a "pull-back" image (more distant) for ectopic thyroid tissue are optional images if a pinhole collimator is not available. **(Pete 2000)**

3.5.2 Dynamic Renal Imaging Techniques (Renogram)

Radiopharmaceutical

• 99mTc-DTPA (diethylenetriaminepentaacetic acid)

Localization

• Compartmental, blood flow

Adult Dose Range

• 99mTc: 3–20 mCi (111–740 MBq) generally 10mCi (370 MBq) for most studies.

Method of Administration

• Bolus intravenous injection

Patient Preparation

• Identify the patient. Verify doctor's order. Explain the procedure.

• Instruct patient to hydrate well (water; up to 10 mL/kg) and void just before test.

• Post study voiding is recommended to lessen bladder exposure.

Procedure (VARIES GREATLY; TIME: ~30

• If GFR is to be included, count the syringe before and after injection for 1 minute at 20–30 cm from camera face (use same distance both times).

• Place patient in supine position, camera under table, except for kidney replacement patients for whom camera is placed anterior over the abdomen to include lower abdomen.

• Position camera by point source over xiphoid, umbilicus, pubic symphysis, and sides in field of view.

• Bolus intravenous injection, start camera. Note: some wait until they see activity blush in abdomen (the "umbrella" effect caused by the heart-liver-

spleen and descending aorta) before starting camera. To be sure, set flow for 120 seconds; start camera just before injection.

• Diuretic (furosemide) study, use following options:

• Insert intravenous butterfly with 3-way stopcock, inject furosemide, flush and inject a bolus of radiotracer. Protocols vary for furosemide injection time. Some wait until 10 to 15 minutes for obstruction studies.

• For 1-minute flow: Inject bolus, start camera, inject furosemide, and flush.

    • Acquire statics at 2- to 5-minute intervals for 30 minutes or serial (dynamic) 1-minute images for 30 minutes. (Most systems have a preset for renogram, renal qualitative or renal perfusion.) **(Pete 2000)**

3.5.3 Bone Scan

Radiopharmaceutical

• MDP (methylene diphosphonate).

Adult Dose Range

• 20–30 mCi (740–1110 MBq), pediatrics by weight.

Method of Administration

• Intravenous.

Patient Preparation

- Identify the patient. Verify doctor's order. Explain the procedure.
- For flow of three phase bone study; remove any attenuating material from region of interest (ROI).
- Instruct patient to drink lots of fluids (hydrate well) and urinate often before imaging.
- Instruct patient to return in 2–4 hours (usually 3 hours) after injection for delayed statics, whole body imaging or SPECT.

Procedure (Time: Immediate Flows, ~10 Minutes; Scans, Acquired 2–4 Hours [Usually 3 Hours] After Injection; Images Take 20–60 Minutes)

- Instruct patient to empty bladder, empty pockets, remove jewelry and necklaces, check pants and shirts for buttons, external prosthesis, braces, etc., anything that can cause artifacts and attenuation.
- Remove cardiac monitors from field of view (FOV).
- Note location of pacemaker, pumps, colostomy bags, etc.
  For whole body scan, position patient supine (although prone, sitting, or standing is not uncommon), arms at side, with knee pillow and foot band (if protocol). **(Pete 2000)**

Chapter Four

Results

4.1 Result

Table 4.1.1 shows gender frequency for all patients

Gender	Frequency	Percent
Female	85	52.8%
Male	76	47.2%
Total	161	100.0%

Table 4.1.2 shows statistical parameter for thyroid scan for all patients

Variables	***Mean***	***Median***	***STD***	***Min***	***Max***
Age	12.26	14	3.65	0.2	15
High	1.43	1.49	.20	0.8	1.7
Weight	41.87	44.5	16.56	10	82
Activity	2.89	2.8	1.12	0.5	5.2
Rec A	1.38	1.49	.46	0.4	2.1
ED RADAR 2018	1.92	1.7	.81	0.7	4.8
ED ICRP 128	2.27	1.9	1.0	0.8	6.2
Avg ED	2.09	1.8	.90	0.8	5.5

Table 4.1.3 shows statistical parameter for dynamic renal scan for all patients

Variables	*Mean*	*Median*	*STD*	*Min*	*Max*
Age	6.55	5.50	4.83	1	15
High	1.09	1.16	0.37	0.5	1.7
Weight	24.01	19	18.19	3.9	96.5
Activity	2.41	2.15	0.88	1	5
Rec A	2.78	2.65	1.1	1	5.3
ED RADAR 2018	0.72	0.8	0.19	0.3	1.1
ED ICRP 128	0.82	0.75	0.2	0.5	1.5
Avg ED	0.77	0.75	0.16	0.45	1.15

Table 4.1.4 shows statistical parameter for bone scan to all patient

Variables	*Mean*	*Median*	*STD*	*Min*	*Max*
Age	11	12	4.12	3	15
High	1.4	1.42	0.19	0.9	1.7
Weight	33.64	35	14.3	12	71
Activity	11.46	12	3.46	5.8	17
Rec A	7.22	7.57	2.63	3	13.2
ED RADAR 2018	3.1	3	0.61	1.9	5.2
ED ICRP 128	3.68	3.6	0.73	2.3	6.1
Avg ED	3.4	3.3	0.66	2.1	5.5

Table 4.1.5 shows the average of effective dose to patients according to their age

Age Group	Thyroid	Dynamic renal scan with DTPA	Bone
1-3	1.2	0.73	3.45
4-8	2.84	0.80	3.32
9-13	2.22	0.82	3.35
14-17	1.85	0.76	3.45

Table 4.1.6 shows the comparison between present study with other according to ED

	Thyroid	Dynamic renal scan with DTPA	Bone
Present study	2.03	0.78	3.39
Silvia Maria 2014	1.2	0.35	2.75
ARPANSA 2008	2.2	6	5.5
LITHUANIA 2012	0.51	0.36	2.79

Table 4.1.7 shows comparison between present study with other studies according to administered activity

	Thyroid	**Dynamic renal scan with DTPA**	**Bone**
Present study	106.93	89.17	430.68
LITHUANIA 2012	92	108	517
JAPAN 2015	300	70	950
SSK 2000	-	150	750
Ireland 2004	80	300	600
EC 99	10	20	40
Malaysia 2010	202	294	574

Chapter Five
Discussion, Conclusion and Recommendations

5.1Discussion

Estimate of effective dose for pediatric in Khartoum state for three nuclear medicine scan the thyroid, dynamic renal scan and bone were **Table 4.1.1** show gender frequency where the number of females was 85 patient with 52%, for males the number was 76 with 47%.

Table 4.1.2 shows statistical parameter for thyroid scan to all patient where the data presented as mean ± standard deviation, where for age the mean was 12.26±3.65 years, for height the mean was 1.43±0.20 cm, for weight the mean was 41.87±16.56 kg, for activity the mean was 2.89±1.12 mci, for recommended activity the mean was 1.38±.46 mci, for effected dose calculated by RADAR 2018 the mean was1.92±0.81 mSv, for the effected dose calculated by ICPR 128 the mean was 2.27±1.0 mSv and for the average effected dose the mean was 2.09±0.90 mSv.

Table 4.1.3 shows statistical parameter for dynamic renal scan to all patient where the data presented as mean ± standard deviation, where for age the mean was 6.55±4.83 years, for height the mean was 1.09±0.37 cm, for weight the mean was 24.01±18.19 kg, for activity the mean was 2.41±0.88 mci, for recommended activity the mean was 2.78±1.1 mci, for effected dose calculated by RADAR 2018 the mean was 0.72±0.19 mSv, for the effected dose calculated by ICPR 128 the mean was 0.82±0.2 mSv and for the average effected dose the mean was 0.77±0.16 mSv.

Table 4.1.4 shows statistical parameter for bone scan to all patient where the data presented as mean ± standard deviation, where for age the mean was 11±4.12 years, for height the mean was 1.4±0.19 cm, for weight the mean was

33.64±14.3 kg, for activity the mean was 11.46±3.64 mci, for recommended activity the mean was 7.22±2.63 mci, for effected dose calculated by RADAR 2018 the mean was 3.1±0.61 mSv, for the effected dose calculated by ICPR 128 the mean was 3.68±2.3 mSv and for the average effected dose the mean was 3.4±0.66 mSv.

The average of effective dose to all patients according to their age, for age group from 1-3 years old the mean for thyroid was 1.2 mSv, for dynamic renal scan 0.73 mSv and for bone scan it was 3.45 mSv. For age group 4-8 years old the mean for thyroid was 2.84 mSv, for dynamic renal scan 0.80 mSv and for bone scan it was 3.32 mSv. For age group 9-13 years old the mean for thyroid was 2.22 mSv, for dynamic renal scan 0.82 mSv and for bone scan it was 3.35 mSv. For age group 14-17 years old the mean for thyroid was 1.85 mSv, for dynamic renal scan 0.76 mSv and for bone scan it was 3.45 mSv in **Table 4.1.5.**

Table 4.1.6 shows the comparison between present study with other studies according to ED where for thyroid the present study was 2.03 mSv while in ARPANSA 2008 study it was 2.2 mSv which consider higher than our present study. For dynamic renal scan present study was 0.78 mSv while in ARPANSA 2008 study was 6 mSv which consider higher than our present study. For bone present study was 3.39 mSv while in ARPANSA 2008 study was 5.5 mSv which consider higher than our present study.

Table 4.1.7 shows comparison between present study with other studies according to administered activity

5.2 Conclusion:

The average of effective dose to all patients according to their age, for age group from 1-3 years old the mean for thyroid was 1.2 mSv, for dynamic renal scan 0.73 mSv and for bone scan it was 3.45 mSv. For age group 4-8

years old the mean for thyroid was 2.84 mSv, for dynamic renal scan 0.80 mSv and for bone scan it was 3.32 mSv. For age group 9-13 years old the mean for thyroid was 2.22 mSv, for dynamic renal scan 0.82 mSv and for bone scan it was 3.35 mSv. For age group 14-17 years old the mean for thyroid was 1.85 mSv, for dynamic renal scan 0.76 mSv and for bone scan it was 3.45 mSv.

And the comparison between present study with other studies according to ED where for thyroid the present study was 2.03 mSv while in ARPANSA 2008 study it was 2.2 mSv which consider higher than our present study. For dynamic renal scan present study was 0.78 mSv while in ARPANSA 2008 study was 6 mSv which consider higher than our present study while in Silvia Maria 2014 study was 0.75 mSv which consider lower than our present study. For bone present study was 3.39 mSv while in ARPANSA 2008 study was 5.5 mSv which consider higher than our present study.

5.3 Recommendations:

- Increase numbers of patients to get more accurate results.
- More hospitals and centers.
- Find better methods to calculate the activity for patients.
- Follow the IAEA recommendations when dealing with radioactive materials.

5.4 Reference

1. **Amir Shahzad** on Introductory Chapter: Role of Nuclear Medicine in Medical Science, 2019.
2. **Donald P. Frush** on Radiation risks to children from medical imaging, 2013.
3. **Frederic H. Fahey, S. Ted Treves, S. James Adelstein** on Minimizing and Communicating Radiation Risk in Pediatric Nuclear Medicine, 2011.
4. **Frederic H. Fahey, Henry Hee-Seong Bom, turo Chiti, Yun Young Cho, Gang Huang, Michael Lassmann, Norman Laurin, Fernando Mut, Rodolfo Nuñez-Miller, Darin O'Keeffe, Prasanta Pradhan, Andrew M. Scott, Shaoli Song, Nischal Soni, Mayuki Uchiyama and Luis Vargas on** Standardization of Administered Activities in Pediatric Nuclear Medicine: A Report of the First Nuclear Medicine Global Initiative Project, Part 1—Statement of the Issue and a Review of Available Resources, 2015.
5. **Frederic H. Fahey, Alison B. Goodkind, Donika Plyku, Kitiwat Khamwan, Shannon E. O'Reilly, Shannon E. O'Reilly, Eric C. Frey, Ye Li, Wesley E. Bolch, George Sgouros, S. Ted Treves on** Dose Estimation in Pediatric Nuclear Medicine, 2016.
6. **Jeffry A. Siegel, Bill Sacks, Charles W. Pennington, James S. Welsh on** Dose Optimization to Minimize Radiation Risk for Children Undergoing CT and Nuclear Medicine Imaging Is Misguided and Detrimental, 2017.
7. **Kristy R. Kutanzi, Annie Lumen , Igor Koturbash , Isabelle R Miousse** on Pediatric Exposures to Ionizing Radiation: Carcinogenic Considerations, 2016.
8. **Lars Johansson** on Principles of Translational Science in Medicine (Second Edition), 2015.
9. **Lassmann M, Biassoni L, Monsieurs M, Franzius** C; EANM Dosimetry and Paediatrics Committees. The new EANM paediatric dosage card: additional notes with respect to F-18. Eur J Nucl Med Mol Imaging. 2008 Sep;35(9):1666-8. doi: 10.1007/s00259-008-0799-9. Epub 2008 Jun 24. Erratum in: Eur J Nucl Med Mol Imaging. 2008 Nov;35(11):2141
10. **M. Lassmann, S.T.Treves. Pediatric Radiopharmaceutical Administration: Harmonization of the 2007** EANM Paediatric Dosage Card (Version 1.5.2008) and the 2010 North America Consensus guideline, Eur J Nucl Med Mol Imaging. 2014, DOI: 10.1007/s00259-014-2731-9.

11. **National Academies Press (US) on** National Research Council (US) Committee on Medical Isotope Production without Highly Enriched Uranium, 2009.
12. **Pete** on Nuclear Medicine Technology: Procedures and Quick Reference, 2nd Edition, 2000.
13. **Peter F. Sharp, Howard G. Gemmel, Alison D. Murray on** Practical Nuclear Medicine, Third Edition, 2005.
14. **Richard M. Shore, William R. Hendee on** Radiopharmaceutical Dosage Selection for Pediatric Nuclear Medicine, 1986.
15. **Sten Carlson** on A Glance At The History Of Nuclear Medicine, 2005**.**
16. **Wall and Hart, Brit J Radiol, 1997**, UNSCEAR 2000 or the 2007 CRCPD NEXT report; most pharmaceutical doses taken from ICRP Publications 53 and 80.
17. **World Health Organization** on Communicating Radiation Risks in Pediatric Imaging, 2016**.**
18. **ED BY RADAR 2017 & ICRP 128**
http://www.snmmi.org/ClinicalPractice/doseTool.aspx?ItemNumber=11216&navItemNumber=11218
19. **Recommended Dose**
https://www.eanm.org/publications/dosage-calculator/

APPENDIX

Gender	Age	Height	Weight	Dose